

Compact Rule-Based Classifier Learning via Gradient Descent

Javier Fumanal-Idocin^{*1}, Raquel Fernandez-Peralta², and Javier Andreu-Perez¹

¹School of Computer Science and Electronic Engineering, University of Essex, Essex, United Kingdom

²Slovak Academy of Sciences, Bratislava, Slovakia

Abstract

Rule-based models play a crucial role in scenarios that require transparency and accountable decision-making. However, they primarily consist of discrete parameters and structures, which presents challenges for scalability and optimization. In this work, we introduce a new rule-based classifier trained using gradient descent, in which the user can control the maximum number and length of the rules. For numerical partitions, the user can also control the partitions used with fuzzy sets, which also helps keep the number of partitions small. We perform a series of exhaustive experiments on 40 datasets to show how this classifier performs in terms of accuracy and rule base size. Then, we compare our results with a genetic search that fits an equivalent classifier and with other explainable and non-explainable state-of-the-art classifiers. Our results show how our method can obtain compact rule bases that use significantly fewer patterns than other rule-based methods and perform better than other explainable classifiers.

1 Introduction

Deep neural networks (DNNs) have been used to solve complex problems in machine learning where non-structured data is available in large volumes, such as image and video [LeCun et al., 2015]. However, the use of these models is not always possible in cases where human liability is still relevant in the decision-making process, like medicine and finance [Arrieta et al., 2020]. Rule-based algorithms are considered one of the most trustworthy for the users, as they explicitly tell the users the patterns found and their relevance in each decision. They are also considered more faithful than other post hoc explainable artificial

*Corresponding author: j.fumanal-idocin@essex.ac.uk

intelligence (XAI) methods, which are not always reliable [Molnar, 2020, Tomsett et al., 2020].

By studying the rules themselves, practitioners can find additional clues about a problem, and they can also disregard the patterns found by the classifier that are contrary to existing knowledge [Li et al., 2024]. It is also a popular use case for rule-based inference to use the rule base as a proxy for a more complicated model, such as a deep learning model, to perform post hoc explanations [Zhang et al., 2018, Li et al., 2024]. One of the main research topics in rule-based classification is the trade-off between interpretability and accuracy, as the larger the number of rules, the less interpretable the model becomes. For example, ensembles of tree-based models usually perform very well, at the cost of losing the interpretation capabilities that a single tree has [Breiman, 2001, Friedman, 2002]. Bayesian reasoning has also been used, but it usually requires Markov chain models to train them, which is very time-consuming [Wang et al., 2017]. Fuzzy rules have been trained mainly using genetic optimization, which balances accuracy and complexity well but causes significant scaling problems [Alcalá-Fdez et al., 2011]. Pure gradient-based approaches have also been used to train rules [Wang et al., 2024, Zhang et al., 2023]. However, they can result in an arbitrarily high number of additive rules, and the only way to handle the model complexity is to perform a dense search of hyperparameters. In addition, how these models partition the state can also be hard to understand for a possible user, especially when the number of rules is high, as the cut points can be arbitrary and very numerous.

In this work, we develop a rule-based system, named Fuzzy Rule-based Reasoner (FRR), that can be trained exclusively using gradient descent and where we can manually set the number of rules and antecedents. The space partitions that the FRR uses as logic antecedents can also be set so that they are intuitive to the user. To obtain this, our contributions are the following:

- To maximize the **interpretability of the system**: we introduce our method for replicating the discrete operations of rule-based systems with matrix operations where the maximum number of rules, antecedents, and partitions can be set a priori.
- To ensure **training effectiveness and scalability**: we discuss the differentiability issues of the FRR and how to solve them. For that, we propose a relaxation of the indicator function that we call restricted addition, which also boosts the performance of the training process and residual connections for training.
- We show the **superiority of the gradient-based training** with respect to an equivalent rule-based classifier using genetic optimization and against other explainable classifiers in 40 different classification datasets.

2 Related Work

2.1 Rule-based models

Rule-based models and decision trees have been mostly trained using heuristic procedures due to their discrete and non-differentiable nature [Wei et al., 2019]. However, these algorithms may not find the best solution and are not guaranteed to find a close one [Rudolph, 1994]. Search algorithms can also be used, but they are expensive to compute, making them unfeasible in large datasets. Most existing rule-based methods mine a series of frequent patterns, which may not be ideal in all situations and do not achieve the same performance as other complex methods such as gradient boosting or random forest [Yuan, 2017]. However, such complex models are harder to interpret, and it is necessary to use tools such as Shapley values to do so [Lundberg et al., 2020]. Fuzzy rules offer good interpretability, but they are computationally intensive to train [Mendel, 2023] and might require hundreds of rules to achieve good performance.

Rule-based methods have been used as well for explainable symbolic reasoning when the antecedents are known concepts, and their relationships can be exploited to solve tasks such as classification. Logic structures can be fixed, and then the right concepts are to be found [Petersen et al., 2022, Barbiero et al., 2023]. Finding the optimal connections among the concepts studied [Vemuri et al., 2024] is also possible. However, the interpretability of the system is compromised by the quality of the concept detection, which is hard to assess. It is also possible to distil black-box models into rule-based ones with good results Li et al. [2024], at the expense of having to train both models.

2.2 Gradient-based training for rule-based and discrete models

Due to the good scalability of gradient-based optimization, gradient-based methodologies have been developed for many systems that are not directly differentiable. The most popular is the Straight-Through Estimator (STE) [Bengio et al., 2013]. Gumbel-Softmax estimator is also very used in architectures that need to sample a categorical distribution in a differentiable model [Jang et al., 2016], such as variational autoencoders. Gradient-based optimization for discrete models is also closely related to the quantization of a DNN. For example, one of the pioneering works in using binary weights was aimed at reducing the computing expenses of a DNN model [Courbariaux et al., 2015].

The most common approaches to gradient-based rule learning involve the joint use of discrete and continuous models so that continuous models generate a good gradient flow [Wang et al., 2024, Zhang et al., 2023]. The problem in that case is to make sure that the discrete and continuous models behave similarly, which is particularly complex for large models. These models also tend to create large numbers of additive rules, so the reasoning mechanism is very difficult for a human being to understand properly. For the case of fuzzy rule-based inference, it is possible to optimize fuzzy sets using gradient descent

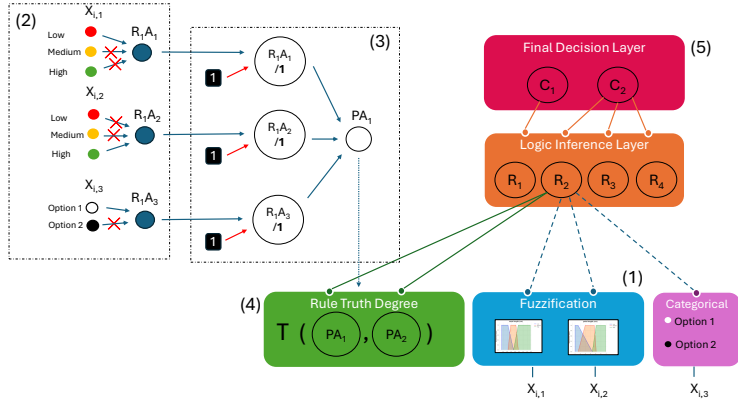


Figure 1: Visual scheme of the Fuzzy Rule-based Reasoner, for example using an input X_i with three features, four rules and two target classes. The inference process is as follows: **(1)** We fuzzify the input for each real-valued variable, obtaining the degree of truth for each linguistic label. For categorical variables, we simply identify the specific value it holds. **(2)** We forward the truth values for each linguistic label and the activated categories in categorical variables to the logic inference layer. This layer selects the linguistic label or category for each antecedent based on the weight magnitudes. We repeat this process for the desired number of antecedents. **(3)** We reduce the size of the rule by determining which antecedents are needed. If an antecedent is not needed, we substitute its truth degree with one, which is the identity element of multiplication. **(4)** We compute the truth value for each rule by multiplying the truth degree of its antecedents. **(5)** We select the output class indicated by the rule with the maximum truth degree. If using additive rules, each rule has a set of weights assigned, which are pondered and then summed based on their truth degrees.

[Mendel, 2023]. However, antecedent search using fuzzy sets is not explored in the literature using gradient-descent methods.

Our method, Fuzzy Rule-based Reasoner (FRR), differs from the previous methods in that it proposes an architecture that performs discrete inference while also being able to specify the maximum number of rules, antecedents, and partitions. In addition, the FRR is trained using only gradient-descent techniques and is able to use both sufficient and additive rules, which also enhances its interpretability.

3 Gradient-based Rule Inference

3.1 General scheme

Let $\mathcal{D} = \{(X_1, Y_1), \dots, (X_N, Y_N)\}$ denote a data set with N instances and M features, where X_i is the observed feature vector of the i -th instance with j -th

entry $X_{i,j}$ and Y_i being its discrete associated target. Each feature can be either discrete or continuous, and the target is a categorical variable with C classes.

The FRR is a rule-based model with L layers of matrix operations. We will denote by $\mathcal{U}^{(l)}$ the l -th layer and by $u_j^{(l)}$ and n_l the j -th node and the total number of nodes in that layer, respectively. The output of the l -th layer is denoted by a vector $\mathbf{u}^{(l)}$ that contains, as instances, the value of each node and $\mathbf{W}^{(l)}$ represents the connectivity matrix of layer l , whose structure and size are specified separately for each layer. We set a \mathbf{W} matrix vector with the connectivity matrices of the different layers for each rule, but we omit this index for the sake of notational simplicity. The components of the FRR are described below and are shown in Figure 1.

3.2 Fuzzification layer

Existing rule-based gradient methods rely on dense binarization of real-valued variables to generate partitions, which are then used as potential antecedents for rule construction. In contrast, the FRR model uses fuzzy logic and fuzzy sets to define partitions that are both significantly simpler and more interpretable for end users.

Fuzzy logic extends classical binary logic by allowing truth values to take any real number within the range $[0, 1]$ Hájek [2013]. Traditional Boolean operators are then replaced with their real-valued counterparts. For example, conjunction (the logical "and") is modelled using T-norms, such as the product or minimum operator, whereas disjunction (the logical "or") is modelled using T-conorms, such as the maximum operator.

The process of fuzzification involves mapping values from the original domain to degrees of membership in fuzzy sets, which collectively form a fuzzy partition. This partitioning divides the universe of discourse into overlapping fuzzy sets, enabling a more nuanced representation of information. Fuzzy partitions are designed to align with linguistic terms such as "low," "medium," or "high" Zadeh [1975]. This linguistic representation allows for a more compact set of partitions in real-valued features. Additionally, linguistic concepts provide greater interpretability for end users, as they correspond more naturally to human reasoning than arbitrary numerical thresholds.

The first layer of the FRR model is a fuzzification block that transforms input observations into degrees of truth according to predefined fuzzy partitions. All numerical features are represented as fuzzy linguistic variables with at most V linguistic labels. Formally, the i -th instance, feature j , and linguistic label v , the degree of truth is denoted by $\mu_{j,v}(X_{i,j})$. So, the output of the fuzzification layer is given by $u_{j+v}^{(1)} = \mu_{j,v}(X_{i,j})$.

Categorical variables are represented using one-hot encoding, which can be interpreted as a degenerate form of fuzzy partitioning, where truth values are restricted to 0 or 1. Consequently, categorical variables can be seamlessly incorporated into the model without additional considerations, as each category is modelled using a degenerated fuzzy set.

3.3 Logic inference layers

We first consider the Mamdani inference expression to compute the truth value of a fuzzy rule r in an inference system

$$r(X) = w_r \prod_{a \in A_r} \mu_a(X), \quad (1)$$

being w_r the rule weight, A_r the set of antecedents of the rule and $\mu_a(X)$ the truth degree of the corresponding fuzzy set.

In order to replicate this, we propose to separate the logic inference into two steps, which correspond to two different layers in the hierarchical model. The first step is to choose which space partitions are forwarded into the rule for each feature. With that aim, layer 2 uses a weight matrix $\mathbf{W}^{(2)}$ of size $M \times V$, i.e., the number of features per number of linguistic labels, which measures the significance of each linguistic label in the logic inference. Then, we only forward the linguistic label with the highest weight value per each feature. In accordance, the output of the second layer is

$$\begin{aligned} u_j^{(2)} &= \sum_{v=1}^V f(W_{j,v}^{(2)}) W_{j,v}^{(2)} u_{j+v}^{(1)} \\ &= \sum_{v=1}^V f(W_{j,v}^{(2)}) W_{j,v}^{(2)} \mu_{j,v}(X_{i,j}), \end{aligned} \quad (2)$$

where f is an indicator function that, given an instance $M_{i,j}$ of the i -row of a certain matrix \mathbf{M} , returns 1 if that instance has the highest value in the row, i.e.,

$$f(M_{i,j}) = \begin{cases} 1 & \text{if } j = \arg \max_k M_{i,k}, \\ 0 & \text{otherwise.} \end{cases} \quad (3)$$

The second step for performing the logic inference is to choose which features are selected as part of the antecedents of the rule. In order to set the number of antecedents per rule to a fixed size A , in the third layer, we use a weight matrix $\mathbf{W}^{(3)}$ of size $A \times M$, which quantifies the relevance of each feature per antecedent in the rule. The contribution of the k -th antecedent is given by the following equation:

$$A_k = \sum_{j=1}^M f(W_{k,j}^{(3)}) W_{k,j}^{(3)} u_j^{(2)}, \quad (4)$$

where f is the function defined in Eq. (3). Consecutively, the degree of truth of each rule is computed as the product of all antecedent's contributions and is the output of the third layer

$$u^{(3)} = \prod_{k=1}^A A_k = \prod_{k=1}^A \sum_{j=1}^M f(W_{k,j}^{(3)}) W_{k,j}^{(3)} u_j^{(2)}. \quad (5)$$

In this step, it can happen that the same antecedent is propagated more than once. In that case, the same membership is powered as many times as it was chosen, which is equivalent to using linguistic hedges in the original partition space [Mendel, 2023].

In order to have a valid fuzzy logic inference process, we need to keep the domain of Eq. (5) inside $[0, 1]$. Since the input values are already in that range and only the multiplication operation is used, it is sufficient to make sure that the weights are also in that range to keep everything in $[0, 1]$. To do so, each weight in Eq. (5) is transformed using the softmax function

$$\tilde{W}_{i,j}^{(l)} = \frac{e^{W_{i,j}^{(l)}/\alpha}}{\sum_m e^{W_{i,m}^{(l)}/\alpha}}, \quad (6)$$

where α is a positive real number called the temperature parameter and controls the sharpness of the distribution. If $\alpha = 1$ we retrieve the standard form of the softmax function. We set in our experiments $\alpha = 0.1$, so that Eq. (6) becomes a better approximation of Eq. (3), which will be relevant when computing the gradients of the model.

To sum up, if we apply the softmax in Eq. (6), resolve the argmax functions in Eqs. (2) and (5) and denote by v_j the space partition of the j -th feature with the highest weight and j_k the feature with the highest weight for the k -th antecedent of the rule we obtain the following expression:

$$r(X_i) = \prod_{k=1}^A \tilde{W}_{k,j_k}^{(3)} \tilde{W}_{j_k,v_{j_k}}^{(2)} \mu_{j_k,v_{j_k}}(X_{i,j_k}). \quad (7)$$

Notice that since all weights lie within $[0, 1]$ the term $\prod_{k=1}^A \tilde{W}_{k,j_k}^{(3)} \tilde{W}_{j_k,v_{j_k}}^{(2)}$ works as w_r in Eq. (1), so the weight of the rule corresponds to the accumulated weight of the relevance of each feature and label selected to be in the antecedent. The other term is the original truth value, i.e., the product of all the membership degrees involved in the rule evaluated to the particular instance.

3.4 Making the model parsimonious

The procedure in Section 3.3 sets the number of antecedents per rule to a fixed value. This number represents the highest possible count of antecedents, but ideally, we aim to keep the number of antecedents limited to ensure rule interpretability and reduce the risk of overfitting. In many cases, concise rules not only enhance performance but also ensure that the model remains easily understandable for human users.

To reduce the number of antecedents in each rule, we make them “compete” with a null element that will make the system ignore the antecedent value if it is not useful. To do so, we can consider the convex combination between 1 and the contribution of each antecedent of the rule

$$\tilde{A}_k = \alpha_k A_k + (1 - \alpha_k), \quad (8)$$

where $\alpha_k \in [0, 1]$. When $\alpha_k = 1$, the value A_k is unmodified, and when $\alpha_k = 0$, $\tilde{A}_k = 1$, which makes this irrelevant for the computation of Eq. (5). Nonetheless, to avoid having only partially cancelled antecedents, we use again the indicator function in Eq. (3) and slightly modify the expression using two weights instead of one

$$\tilde{A}_k = \prod_{k=1}^A (f(\alpha_{k,1})A_k + f(\alpha_{k,2})), \quad (9)$$

where $\alpha_{k,1}, \alpha_{k,2} \in \mathbb{R}$. We can do this after the antecedent has been selected in Eq. (5) by replacing A_k for \tilde{A}_k .

3.5 Final decision layer

This module computes the predictions of the FRR given the truth degrees of the rules. In this layer, we consider the matrix $\mathbf{W}^{(4)}$ of size $R \times C$ where R is the number of rules and C the number of classes of the target variable. Then, each weight $W_{s,c}^{(4)}$ corresponds to the score that rule r_s gives to class c . Taking into account the truth degrees of each rule provided by the previous layer, we can compute the final outcome, denoted in general by $u_c^{(4)}$, using sufficient or additive rules.

- *Sufficient rules*: for a fixed class c we consider the set of rules whose maximum score is assigned to c and then we consider the value of the highest score per truth degree as output

$$FRR(X_i)_c^{suf} = \max_{s \in \{1, \dots, R\}} f(W_{s,c}^{(4)})W_{s,c}^{(4)}r_s(X_i). \quad (10)$$

To select which rules have c as the class with maximum score we use again the function in Eq. (3).

- *Additive rules*: in this case we just perform the standard matrix multiplication between the rules truth degrees and the score matrix

$$FRR(X_i)_c^{ad} = \sum_{s=1}^R W_{s,c}^{(4)}r_s(X_i). \quad (11)$$

Again, we need to apply the softmax function in Eq. (6) to maintain the weights between $[0, 1]$. In this manner, since fuzzy truth degrees are already numbers in $[0, 1]$, we can directly apply the cross-entropy loss \mathcal{L} without further modifications.

Notice that Eqs. (2), (5), (9) and (10) are not differentiable with respect to the weights because of the presence of the argmax function in the definition of f in Eq. (3). We show how to overcome this problem and others related to gradient-based optimization of the FRR in Section 4.

3.6 Extracting the rules from the model

Once trained, we can recover the rules obtained by the system by following “the paths” in the FRR. For each rule, we select the features that have the biggest weights according to $\mathbf{W}^{(3)}$ that were not cancelled in Eq. (9). Then, for each feature we select the linguistic label according to $\mathbf{W}^{(2)}$ and finally, in the decision layer, we choose the consequent according to $\mathbf{W}^{(4)}$ and depending on if we are working with sufficient or additive rules, considering Eq. (10) or (11), respectively.

4 Gradient-based optimization of the FRR

4.1 Component derivation in the FRR

To optimize the cross-entropy loss we consider gradient-based optimization, so the parameters are going to be updated according to

$$\mathbf{W}^{(l)}|_{t+1} = \mathbf{W}^{(l)}|_t - \eta_t \frac{\partial \mathcal{L}}{\partial \mathbf{u}^{(4)}} \cdot \frac{\partial \mathbf{u}^{(4)}}{\partial \mathbf{W}^{(l)}}, \quad (12)$$

where η_t is the learning rate. Then, to ensure an effective update of the model’s parameters, let us analyse the derivative of each node with respect to its directly connected weights and nodes.

First of all, since all the weights are normalized using the softmax function (see Eq. (6)), the derivative of each node according to the weights is multiplied by the derivative of the softmax, i.e.,

$$\frac{\partial u^{(l)}}{\partial W_{i,j}^{(l)}} = \frac{\partial u^{(l)}}{\partial \tilde{W}_{i,j}^{(l)}} \cdot \frac{\partial \tilde{W}_{i,j}^{(l)}}{\partial W_{i,j}^{(l)}},$$

where

$$\frac{\partial \tilde{W}_{i,j}^{(l)}}{\partial W_{i,m}^{(l)}} = \frac{1}{\alpha} \tilde{W}_{i,j}^{(l)} \cdot (\delta_{j,m} - \tilde{W}_{i,m}^{(l)}), \quad (13)$$

and $\delta_{j,m}$ is the Kronecker delta. Then, we can compute the derivative of Eqs. (2) and (5) with respect to the normalized weights directly.

$$\frac{\partial u_j^{(2)}}{\partial \tilde{W}_{j,v}^{(2)}} = \left(\frac{\partial f}{\partial \tilde{W}_{j,v}^{(2)}} \tilde{W}_{j,v}^{(2)} + f(\tilde{W}_{j,v}^{(2)}) \right) u_{j+v}^{(1)}. \quad (14)$$

$$\frac{\partial u_j^{(2)}}{\partial u_{j+v}^{(1)}} = f(\tilde{W}_{j,v}^{(2)}) \tilde{W}_{j,v}^{(2)}. \quad (15)$$

$$\frac{\partial u^{(3)}}{\partial \tilde{W}_{k,j}^{(3)}} = \left(\frac{\partial f}{\partial \tilde{W}_{k,j}^{(3)}} \tilde{W}_{k,j}^{(3)} + f(\tilde{W}_{k,j}^{(3)}) \right) u_j^{(2)} \cdot \prod_{\substack{1 \leq m \leq A \\ m \neq k}} \sum_{n=1}^M f(\tilde{W}_{m,n}^{(3)}) \tilde{W}_{m,n}^{(3)} u_n^{(2)}. \quad (16)$$

$$\frac{\partial u^{(3)}}{\partial u_j^{(2)}} = \sum_{k=1}^A f(\tilde{W}_{k,j}^{(3)}) \tilde{W}_{k,j}^{(3)} \prod_{\substack{1 \leq m \leq A \\ m \neq k}} \sum_{n=1}^M f(\tilde{W}_{m,n}^{(3)}) \tilde{W}_{m,n}^{(3)} u_n^{(2)}. \quad (17)$$

By the visual inspection of the derivatives, it is clear that there are several issues to overcome for an efficient training:

- The derivatives in Eqs. (15) and (17) are 0 whenever the corresponding weight is not chosen by the indicator function f , i.e., when the weight is not the biggest one, then it is not updated. This gradient sparsity may severely affect the speed’s training.
- The derivative of f appears in Eqs. (14) and (16) but f is not differentiable since it is defined using the argmax.
- The derivative of the nodes in which the logic inference is performed, i.e., Eq. (17), involves the product of several terms between $[0, 1]$ which may result in the vanishing gradient problem. Notice that this issue escalates with the maximum number of antecedents A .

The derivatives of the remaining components have a similar behaviour and they are included in Appendix B.

In the following sections we introduce several techniques which overcome the above issues and can ensure an efficient training of the FRR.

4.2 Gradient estimation

To compute the derivative of function f , present in numerous equations in the FRR, we have considered gradient estimators, which substitute the derivative of the non-differentiable function by an approximation. This approximation is typically the derivative of the identity function (STE) or another smooth function which behaves similarly to the original Yin et al. [2019]. In the case of the FRR, we replace the derivative of f in Eqs. (14) and (16) by 0 or the identity. Although other approximators could be considered as gradient estimators, there is no guarantee of better results with respect to the use of the identity function Schoenbauer et al. [2024].

Apart from STE, we have also considered “gradient grafting” Wang et al. [2024], which consists of training simultaneously a discrete model in the forward pass and a continuous one in the backward pass.

4.3 Restricted additive contributions

The FRR mimics the behaviour of fuzzy logic inference because of the different indicator functions used during the inference process. However, these functions present some problems. First, they are not differentiable, and we need to use a STE. Secondly, even with the STE, the indicator functions reduce the flow of information to only one of the possible paths. In order to speed up training, we propose a relaxed version of the indicator function during training time that will also keep the standard behaviour of the model in inference mode. Let \mathbf{M} be a matrix of size $n \times m$, we define:

$$f_\beta(M_{i,j}) = \begin{cases} \frac{1}{1+\beta(m-1)} & \text{if } j = \arg \max_k M_{i,k}, \\ \frac{\beta}{1+\beta(m-1)} & \text{otherwise,} \end{cases} \quad (18)$$

where $\beta \in [0, 1]$ is a hyperparameter of the model. In this way, when $\beta > 0$, the additive nature of the summations is restricted but not completely ignored. When $\beta = 0$, Eq. (18) is equivalent to a hard indicator function. Since $\sum_{j=1}^m f_\beta(M_{i,j}) = 1$ always holds regardless of the value of β , the output will not change the scale of the input values.

To set the value β during training, we start with a maximum value (usually 1) and gradually decrease it to a minimum value (usually 0). This allows the model to explore freely with larger gradient flows initially and resemble final inference behavior in later epochs.

4.4 Projection functions

The FRR might find problems of vanishing gradient because the truth degree of a rule is computed using the product of values in the $[0, 1]$ range, which might result in values very close to 0 in Eq. (17). A feasible solution is to use custom functions to slow down the speed of approaching to zero. In Wang et al. [2024] the authors came across a very similar problem, and they propose to use the following function:

$$P(x) = \frac{1}{1 - \log(x)}.$$

However, there are many other functions, like $P(x) = \sqrt{x}$, that would serve the same purpose.

In the case of the FRR, this function can be applied when computing the rule truth degree in Eq. (5)

$$\tilde{u}^{(3)} = \prod_{k=1}^A P(A_k + \varepsilon), \quad (19)$$

with ε a positive small constant.

4.5 Residual connections

We also incorporate a residual connection to tackle the problem with the vanishing gradient in Eq. (5). We consider another connection between the rules output and their antecedent values, similar to residual connections [He et al., 2016]:

$$\tilde{u}^{(3)} = u^{(3)} + \gamma \sum_{k=1}^A A_k. \quad (20)$$

The multiplying constant γ of this expression starts at 0.1 and decreases linearly with the number of epochs passed in the training process, reaching 0 at the end and in the inference process.

5 Experiments

5.1 Experimental settings

We took 40 datasets of different sizes, all of which are very common in studying classification performance. They range from 80 to 19020 samples and from 2 to 85 for different numbers of features. Please take a look at Appendix D to see their specific details and citations. As a performance metric, we use the standard accuracy metric. We use a 5-fold evaluation to obtain more reliable results than a traditional 80/20 split. When evaluating tree and rule-based models, we also measure the number of rules and antecedents they use to solve the problems.

For the fuzzification of real-valued variables, we use 3 linguistic labels, which are translated to the concepts of “low”, “medium” and “high”. The parameters for each of them are computed based on the quantile distribution. See more details about this in the Appendix A.

5.2 Comparison with an equivalent classifier optimized with genetic fine-tuning

We fitted different fuzzy rule-based classifiers using genetic optimization, which is the current state-of-the-art for such systems. We fit classifiers with different number of rules and antecedents, and we found that the best classifiers with this technique were obtained using smaller models (detailed results are shown in Appendix E).

Then, we trained an FRR using the equivalent maximum number of rules, antecedents, and the same linguistic variables to find the best genetic one. The results for both are in Table 1 under the “FRR” and the “FGA” columns. We can see there that the FRR obtained a significant improvement in terms of accuracy over the FGA, backed by a t-test with $p < 0.01$. The number of rules was also bigger, but if we consider both the number of rules and antecedents, we see that the FRR resulted in less complex classifiers (Figure 2).

5.3 Scaling the size of the FRR

Although the ideal FRR should be as compact as possible, we also believe that it is good to be able to scale the model to more complexity if the trade-off of performance is considered worth it by the user.

Just as with genetic optimization, we found problems in scaling the FRR to larger numbers of rules. However, we also found that using additive rules instead of sufficient rules allowed the system to scale better in terms of performance, as can be seen in Figure 2 and Table 1 under the label of AdFRR.

5.4 Classification performance and comparison with other explainable and standard classifiers

Table 1: 5-fold accuracy results for all the datasets considered. We also show the average number of rules used for rule-based models. Models before the vertical bar are those considered interpretable.

| Method | AdFRR | FRR | FGA | RRL | CART | C4.5 | LR | SVM | MLP | RF | GB |
|----------------------|-------|-------|-------|-------|-------|--------|-------|-------|-------|-------|-------|
| Accuracy | 78.00 | 76.90 | 70.46 | 82.33 | 80.67 | 76.87 | 82.22 | 83.51 | 82.84 | 85.87 | 83.94 |
| Number of Rules | 32.32 | 13.77 | 7.12 | 99.85 | 39.75 | 131.92 | - | - | - | - | - |
| Antecedents per Rule | 1.32 | 1.94 | 2.23 | 8.43 | 5.75 | 8.10 | - | - | - | - | - |

Table 1 shows the results for all the datasets and all the classifiers tested. The interpretable methods chosen were: an equivalent Fuzzy Rule Based classifier using genetic fine tuning Fumanal-Idocin and Andreu-Perez [2024] (FGA), Rule-based Representation Learning (RRL), which is another method to obtain gradient optimized rules [Wang et al., 2021], classification trees constructed using Classification and Regression Trees (CART) methodology [Timofeev, 2004], C4.5 Quinlan [1993] and a Linear Regression (LR). We also show results for four models considered “complex”: a Support Vector Machine (SVM), a Multilayer Perceptron (MLP) [Hackeling, 2017], Random Forest (RF) [Ho, 1995] and Gradient Boosting (GB) [Friedman, 2001], being the latter two ensemble models.

In terms of accuracy, the best explainable classifier obtained was the RRL, with an average accuracy of 82.33. It did so, however, but using the largest number of additive rules and antecedents per rule, which makes it hardly interpretable in practice.

In terms of the number of rules, the FRR was only surpassed by the Genetic fine-tuning of the fuzzy rule inference, which performed significantly worse than the FRR in terms of accuracy. The most direct competitor of the FRR, the RRL, obtained more accuracy at the expense of using more than 7 times the number of rules, which are also additive and less interpretable than the FRR sufficient rules. The AdFRR obtained better results than the FRR and the C4.5. An example of a rule base obtained with the FRR is shown in Figure 3.

We believe that all the classifiers that used fuzzy sets were limited in performance by the fuzzification method used, which prioritized explainability over performance. It is also worth pointing out that the performance of any of the

explainable classifiers did not surpass the performance of complex classifiers, which shows that there is still a lot of room to improve for explainable classifiers.

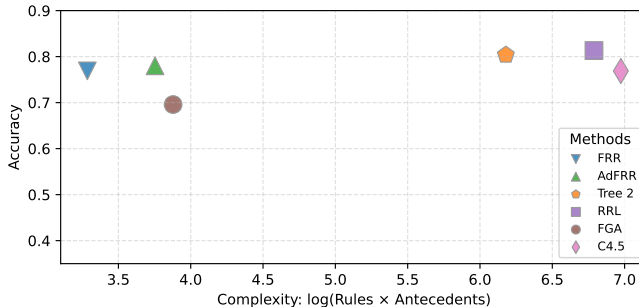


Figure 2: Relation between classifier complexity in terms of antecedents and rules and classifier performance for those classifier where it applies.

5.4.1 Ablation study

To show the effect of the gradient estimation methods in the training process, we also run the FRR with different configurations:

- For the indicator in training: we use the standard indicator, the restricted additions and no indicator.
- With and without residual connections.
- For gradient estimation: STE_0 , approximating the gradient of the indicator with 0, STE_1 likewise with the identity function, and using gradient grafting in substitution of the STE method [Wang et al., 2021].

The results are shown in Table 2, which shows that the residual connections were instrumental in achieving good results. Restricted additions were particularly effective when combined with gradient grafting. For results of more combinations of parameters, we refer the reader to Appendix G.

6 Conclusions and future work

We introduced a new explainable classifier, named Rule-based Fuzzy Reasoner (FRR), that can automatically learn rules for data representation and classification using gradient-based optimization. The FRR comes with a big advantage over other rule-based methods: the user can set the number maximum number of rules and their length, which avoids common problems in real-life applications like having an excessive number of rules and antecedents and overly complex partitions of the space. The FRR presented a series of problems in non-differentiable functions and vanishing gradients, which we studied and mitigated. As tested in the experimentation, the FRR can obtain good performance results both for

Table 2: Results for the ablation study of the compact FRR using different gradient strategies.

| Indicator | Res. connections | Grad. Strategy | Accuracy |
|------------|------------------|------------------|--------------|
| Continuous | No | STE ₀ | 55.52 |
| Standard | No | STE ₀ | 73.52 |
| Standard | Yes | STE ₀ | 76.90 |
| Standard | No | STE ₁ | 73.80 |
| Continuous | No | STE ₁ | 73.89 |
| Standard | Yes | STE ₁ | 76.62 |
| Continuous | Yes | STE ₁ | 76.71 |
| Restricted | No | Graft | 74.08 |
| Continuous | No | Graft | 72.81 |
| Restricted | Yes | Graft | 76.78 |
| Continuous | Yes | Graft | 75.97 |

| Rules for Non-Diabetic Patients |
|---|
| IF Diabetes Pedigree IS Low AND Age IS Low |
| IF Skin Thickness IS Low AND Insulin IS Medium |
| IF Body Mass Index (BMI) IS Low |
| IF Blood Pressure IS High AND Insulin IS Low |
| IF Times Pregnant IS Medium AND |
| Blood Pressure IS High AND Age IS Medium |
| Rules for Diabetic Patients |
| IF Glucose Level IS High |

Figure 3: Classification Rules for the *Pima Indians Diabetes* Dataset Smith et al. [1988].

sufficient and additive rules. Going forward, we aim to study novel fuzzification methods that can retain interpretability while offering better performance. Also, we aim to use the FRR inside bigger deep learning frameworks so that it can offer rule-based explanations of these model’s predictions within the same gradient flow.

7 Acknowledgements

Javier Fumanal-Idocin research has been supported by the European Union and the University of Essex under a Marie Skłodowska-Curie YUFE4 postdoc action. Raquel Fernandez-Peralta is funded by the EU NextGenerationEU through the Recovery and Resilience Plan for Slovakia under the project No. 09I03-03-V04-00557.

The authors acknowledge the use of the High Performance Computing Facility (Ceres) and its associated support services at the University of Essex in the completion of this work.

References

- Jesús Alcalá-Fdez, Rafael Alcalá, and Francisco Herrera. A fuzzy association rule-based classification model for high-dimensional problems with genetic rule selection and lateral tuning. *IEEE Transactions on Fuzzy systems*, 19(5): 857–872, 2011.
- Alejandro Barredo Arrieta, Natalia Díaz-Rodríguez, Javier Del Ser, Adrien Bennetot, Siham Tabik, Alberto Barbado, Salvador García, Sergio Gil-López, Daniel Molina, Richard Benjamins, et al. Explainable artificial intelligence (xai): Concepts, taxonomies, opportunities and challenges toward responsible ai. *Information fusion*, 58:82–115, 2020.
- Pietro Barbiero, Gabriele Ciravegna, Francesco Giannini, Mateo Espinosa Zarlenga, Lucie Charlotte Magister, Alberto Tonda, Pietro Lió, Frederic Precioso, Mateja Jamnik, and Giuseppe Marra. Interpretable neural-symbolic concept reasoning. In *International Conference on Machine Learning*, pages 1801–1825. PMLR, 2023.
- Yoshua Bengio, Nicholas Léonard, and Aaron Courville. Estimating or propagating gradients through stochastic neurons for conditional computation. *arXiv preprint arXiv:1308.3432*, 2013.
- Leo Breiman. Random forests. *Machine learning*, 45:5–32, 2001.
- Matthieu Courbariaux, Yoshua Bengio, and Jean-Pierre David. Binaryconnect: Training deep neural networks with binary weights during propagations. *Advances in neural information processing systems*, 28, 2015.
- Jerome H Friedman. Greedy function approximation: a gradient boosting machine. *Annals of statistics*, pages 1189–1232, 2001.
- Jerome H Friedman. Stochastic gradient boosting. *Computational statistics & data analysis*, 38(4):367–378, 2002.
- Javier Fumanal-Idocin and Javier Andreu-Perez. Ex-fuzzy: A library for symbolic explainable ai through fuzzy logic programming. *Neurocomputing*, page 128048, 2024. ISSN 0925-2312.
- Francesco Giannini, Michelangelo Diligenti, Marco Maggini, Marco Gori, and Giuseppe Marra. T-norms driven loss functions for machine learning. *Applied Intelligence*, 53(15), 2023.
- Gavin Hackeling. *Mastering Machine Learning with scikit-learn*. Packt Publishing Ltd, 2017.

- Petr Hájek. *Metamathematics of fuzzy logic*, volume 4. Springer Science & Business Media, 2013.
- Kaiming He, Xiangyu Zhang, Shaoqing Ren, and Jian Sun. Deep residual learning for image recognition. In *Proceedings of the IEEE conference on computer vision and pattern recognition*, pages 770–778, 2016.
- Tin Kam Ho. Random decision forests. In *Proceedings of 3rd international conference on document analysis and recognition*, volume 1, pages 278–282. IEEE, 1995.
- Eric Jang, Shixiang Gu, and Ben Poole. Categorical reparameterization with gumbel-softmax. *arXiv preprint arXiv:1611.01144*, 2016.
- Markelle Kelly, Rachel Longjohn, and Kolby Nottingham. The uci machine learning repository. URL <https://archive.ics.uci.edu>.
- Yann LeCun, Yoshua Bengio, and Geoffrey Hinton. Deep learning. *Nature*, 521(7553):436–444, 2015.
- Ruoyu Li, Qing Li, Yu Zhang, Dan Zhao, Yong Jiang, and Yong Yang. Interpreting unsupervised anomaly detection in security via rule extraction. *Advances in Neural Information Processing Systems*, 36, 2024.
- Scott M Lundberg, Gabriel Erion, Hugh Chen, Alex DeGrave, Jordan M Prutkin, Bala Nair, Ronit Katz, Jonathan Himmelfarb, Nisha Bansal, and Su-In Lee. From local explanations to global understanding with explainable ai for trees. *Nature machine intelligence*, 2(1):56–67, 2020.
- Jerry M Mendel. *Explainable Uncertain Rule-Based Fuzzy Systems*. Springer, 2023.
- Christoph Molnar. *Interpretable machine learning*. 2020.
- F. Pedregosa, G. Varoquaux, A. Gramfort, V. Michel, B. Thirion, O. Grisel, M. Blondel, P. Prettenhofer, R. Weiss, V. Dubourg, J. Vanderplas, A. Passos, D. Cournapeau, M. Brucher, M. Perrot, and E. Duchesnay. Scikit-learn: Machine learning in Python. *Journal of Machine Learning Research*, 12: 2825–2830, 2011.
- Felix Petersen, Christian Borgelt, Hilde Kuehne, and Oliver Deussen. Deep differentiable logic gate networks. In S. Koyejo, S. Mohamed, A. Agarwal, D. Belgrave, K. Cho, and A. Oh, editors, *Advances in Neural Information Processing Systems*, volume 35, pages 2006–2018. Curran Associates, Inc., 2022.
- J. Ross Quinlan. *C4.5: Programs for Machine Learning*. Morgan Kaufmann, 1993.
- Günter Rudolph. Convergence analysis of canonical genetic algorithms. *IEEE transactions on neural networks*, 5(1):96–101, 1994.

- Matt Schoenbauer, Daniele Moro, Lukasz Lew, and Andrew Howard. Custom gradient estimators are straight-through estimators in disguise, 2024. URL <https://arxiv.org/abs/2405.05171>.
- J.W. Smith, J.E. Everhart, W.C. Dickson, W.C. Knowler, and R.S. Johannes. Using the adap learning algorithm to forecast the onset of diabetes mellitus. In *Proceedings of the Symposium on Computer Applications and Medical Care*, pages 261–265. IEEE Computer Society Press, 1988.
- Roman Timofeev. Classification and regression trees (cart) theory and applications. *Humboldt University, Berlin*, 54, 2004.
- Richard Tomsett, Dan Harborne, Supriyo Chakraborty, Prudhvi Gurram, and Alun Preece. Sanity checks for saliency metrics. In *Proceedings of the AAAI conference on artificial intelligence*, volume 34, pages 6021–6029, 2020.
- Isaac Triguero, Sergio González, Jose M Moyano, Salvador García López, Jesús Alcalá Fernández, Julián Luengo Martín, Alberto Luis Fernández Hilario, María José del Jesús Díaz, Luciano Sánchez, Francisco Herrera Triguero, et al. Keel 3.0: an open source software for multi-stage analysis in data mining. 2017.
- Emile van Krieken, Erman Acar, and Frank van Harmelen. Analyzing Differentiable Fuzzy Logic Operators. *Artificial Intelligence*, 302:103602, 2022.
- Deepika Vemuri, Gautham Bellamkonda, and Vineeth N. Balasubramanian. Enhancing concept-based learning with logic. In *ICML 2024 Workshop on Differentiable Almost Everything: Differentiable Relaxations, Algorithms, Operators, and Simulators*, 2024.
- Tong Wang, Cynthia Rudin, Finale Doshi-Velez, Yimin Liu, Erica Klampfl, and Perry MacNeille. A bayesian framework for learning rule sets for interpretable classification. *Journal of Machine Learning Research*, 18(70):1–37, 2017.
- Zhuo Wang, Wei Zhang, Ning Liu, and Jianyong Wang. Scalable rule-based representation learning for interpretable classification. *Advances in Neural Information Processing Systems*, 34:30479–30491, 2021.
- Zhuo Wang, Wei Zhang, Ning Liu, and Jianyong Wang. Learning interpretable rules for scalable data representation and classification. *IEEE Transactions on Pattern Analysis and Machine Intelligence*, 2024.
- Dennis Wei, Sanjeeb Dash, Tian Gao, and Oktay Gunluk. Generalized linear rule models. In *International conference on machine learning*, pages 6687–6696. PMLR, 2019.
- Penghang Yin, Jiancheng Lyu, Shuai Zhang, Stanley J. Osher, Yingyong Qi, and Jack Xin. Understanding Straight-Through Estimator in Training Activation Quantized Neural Nets. In *International Conference on Learning Representations*, 2019.

- Xiuli Yuan. An improved apriori algorithm for mining association rules. In *AIP conference proceedings*, volume 1820. AIP Publishing, 2017.
- Lotfi Asker Zadeh. The concept of a linguistic variable and its application to approximate reasoning—i. *Information sciences*, 8(3):199–249, 1975.
- Quanshi Zhang, Yu Yang, Ying Nian Wu, and Song-Chun Zhu. Interpreting cnns via decision trees. *2019 IEEE/CVF Conference on Computer Vision and Pattern Recognition (CVPR)*, pages 6254–6263, 2018.
- Wei Zhang, Yongxiang Liu, Zhuo Wang, and Jianyong Wang. Learning to binarize continuous features for neuro-rule networks. In *Proceedings of the Thirty-Second International Joint Conference on Artificial Intelligence*, pages 4584–4592, 2023.

A Computing the fuzzy partitions

For our fuzzy partitions, we use trapezoidal memberships. We chose them instead of Gaussian or other shapes because they are linear functions that are easier to understand for humans. Gaussian shapes are never strictly 0, which can cause unintuitive results sometimes.

The expression for the fuzzy membership takes four parameters:

$$\mu_A(x) = \begin{cases} 0 & \text{if } x \leq a, \\ \frac{x-a}{b-a} & \text{if } a < x \leq b, \\ 1 & \text{if } b < x \leq c, \\ \frac{d-x}{d-c} & \text{if } c < x \leq d, \\ 0 & \text{if } x > d. \end{cases} \quad (21)$$

The parameters a, b, c, d can be easily optimised through gradient as well, but we are not warranted to obtain a reasonable result in that case i.e. lower values in the input space should always have a lower membership value to “high” and “medium” than to “low”. Similarly to ReLU, trapezoidal functions are differentiable everywhere except by four points, which does not cause issues during training.

Our preferred setup is to use 3 linguistic labels, which are translated to the concepts of “low”, “medium” and “high”. The parameters for each of them are computed based on the quantile distribution:

Let \mathbf{X} be a matrix of shape (n, m) where n is the number of samples and m is the number of variables.

1. Compute quantiles: Define quantile percentages: $q_i = \{0, 20, 40, 60, 80, 100\}$
 Compute quantiles: $Q_i = P_{q_i}(\mathbf{X})$, $i = \{0, 1, 2, 3, 4, 5\}$ where $P_q(\mathbf{X})$ is the q -th percentile of each column in \mathbf{X} .
2. Compute partition parameters: Define a tensor \mathbf{P} of shape $(m, 3, 4)$ to store partition parameters.

For the first partition ($i = 0$):

$$\begin{cases} P_{:,0,0} = Q_0 \\ P_{:,0,1} = Q_0 \\ P_{:,0,2} = Q_1 \\ P_{:,0,3} = Q_2 \end{cases}$$

For the second partition ($i = 1$):

$$\begin{cases} P_{:,1,0} = Q_1 \\ P_{:,1,1} = (Q_1 + Q_2)/2 \\ P_{:,1,2} = (Q_2 + Q_3)/2 \\ P_{:,1,3} = Q_3 \end{cases}$$

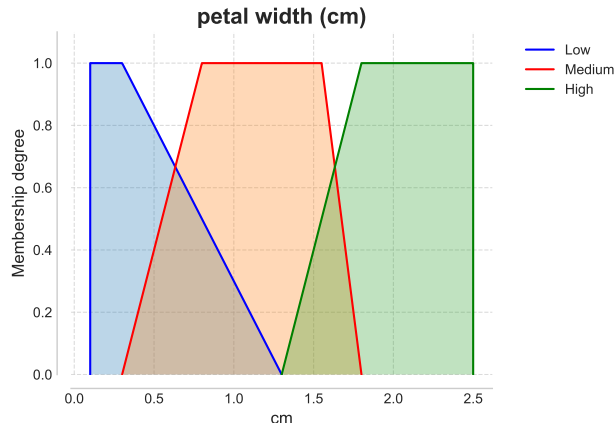


Figure 4: Visualization of fuzzy partitions using the method proposed for the petal width variable in the Iris dataset.

For the third partition ($i = 2$):

$$\begin{cases} P_{:,2,0} = Q_2 \\ P_{:,2,1} = Q_3 \\ P_{:,2,2} = Q_4 \\ P_{:,2,3} = Q_4 \end{cases}$$

The resulting tensor \mathbf{P} contains the trapezoidal parameters for each variable and partition. As a visual example, Figure 4 shows a fuzzy partition computed this way for the classical Iris dataset.

The fuzzy partition itself can be a limiting factor in the performance of the FRR. In order to measure this, we have trained a Multi-Layer Perceptron that takes the membership values to each of the fuzzy partitions as input instead of the original real values, which we can use as an upper estimate of the maximum performance achievable with these partitions. This MLP obtained a 83.32 average accuracy across all datasets, in line with what we obtained with other classifiers. We can take this as an upper threshold of the possible performance possible with the FRR. The MLP is a more flexible model than the FRR and should be able to overperform if properly trained.

Detailed results of the fuzzified-input MLP are in Table 4.

B Remaining gradients of interest

In Section 4, we have included and discussed the derivatives of the second and third layers. For completeness, in this appendix, we compute the rest of the

derivatives involved in the gradient-based optimization of the FRR. Here we already consider the normalized weights.

To compute the derivatives of the fourth and last layer in which the classification step is performed we have to distinguish between the cases of sufficient and additive rules:

- *Sufficient rules:* in this case, for simplifying the notation we consider $h_s(W_{s,c}^{(4)}, r_s) = f(W_{s,c}^{(4)})W_{s,c}^{(4)}r_s(X_i)$, then $u_c^{(4)} = \max_{s \in \{1, \dots, R\}} h_s(W_{s,c}^{(4)}, r_s)$ and we have

$$\frac{\partial u_c^{(4)}}{\partial r_s} = \begin{cases} f(W_{s,c}^{(4)})W_{s,c}^{(4)} & \text{if } s = \arg \max_k h_k, \\ 0 & \text{otherwise.} \end{cases} \quad (22)$$

$$\frac{\partial u_c^{(4)}}{\partial W_{s,c}^{(4)}} = \begin{cases} \left(\frac{\partial f}{\partial W_{s,c}^{(4)}} W_{s,c}^{(4)} + f(W_{s,c}^{(4)}) \right) r_s(X_i) & \text{if } s = \arg \max_k h_k, \\ 0 & \text{otherwise.} \end{cases} \quad (23)$$

Similarly than the discussion in Section 4, Eq. (22) is 0 whenever $W_{s,c}^{(4)}$ is not the biggest score, which blocks the gradient of the corresponding rule, and in Eq. (23) we have to use a gradient estimator since f is not differentiable.

- *Additive rules:*

$$\frac{\partial u_c^{(4)}}{\partial r_s} = W_{s,c}^{(4)}, \quad \frac{\partial u_c^{(4)}}{\partial W_{s,c}^{(4)}} = r_s(X_i). \quad (24)$$

In this case the derivatives correspond to the score and the truth degree, respectively.

Next, we study how the different complementary components of the FRR affect the gradient-based optimization. First, we compute the derivatives involved in the update of the parameters in charge of reducing the number of conditions in each rule (see Eq. (9)):

$$\frac{\partial \tilde{A}_k}{\partial A_k} = f(\alpha_{k,1}) \prod_{\substack{1 \leq m \leq A \\ m \neq k}} f(\alpha_{m,1}) A_m + f(\alpha_{m,2}). \quad (25)$$

$$\frac{\partial \tilde{A}_k}{\partial \alpha_{k,1}} = \frac{\partial f}{\partial \alpha_{k,1}} A_k \prod_{\substack{1 \leq m \leq A \\ m \neq k}} f(\alpha_{m,1}) A_m + f(\alpha_{m,2}). \quad (26)$$

$$\frac{\partial \tilde{A}_k}{\partial \alpha_{k,2}} = \frac{\partial f}{\partial \alpha_{k,2}} \prod_{\substack{1 \leq m \leq A \\ m \neq k}} f(\alpha_{m,1}) A_m + f(\alpha_{m,2}). \quad (27)$$

These derivatives have a similar behaviour that the ones already discuss because of the presence of function f . Next, the derivative of the projection function is

taken into account when the third layer is modified as in Eq. (19):

$$\frac{dP}{dx} = \frac{1}{x(1 - \log(x))^2}. \quad (28)$$

Finally, the derivative of the third layer after including the residual connection is modified additively by the sum of derivatives of the antecedents weighted by γ :

$$\frac{\partial \tilde{u}^{(3)}}{\partial u_j^{(3)}} = \frac{\partial u_j^{(3)}}{\partial u_j^{(2)}} + \gamma \sum_{k=1}^A \frac{\partial A_k}{\partial u_j^{(2)}} = \frac{\partial u_j^{(3)}}{\partial u_j^{(2)}} + \gamma \sum_{k=1}^A f(W_{k,j}^{(3)}) W_{k,j}^{(3)}. \quad (29)$$

$$\frac{\partial \tilde{u}^{(3)}}{\partial W_{k,j}^{(3)}} = \frac{\partial u_j^{(3)}}{\partial W_{k,j}^{(3)}} + \gamma \sum_{k=1}^A \frac{\partial A_k}{\partial W_{k,j}^{(3)}} = \frac{\partial u_j^{(3)}}{\partial W_{k,j}^{(3)}} + \gamma \sum_{k=1}^A \left(\frac{\partial f}{\partial W_{k,j}^{(3)}} W_{k,j}^{(3)} + f(W_{k,j}^{(3)}) \right) u_j^{(2)}. \quad (30)$$

C Using the FRR with other conjunctions

In fuzzy logic, T-norms are considered to be the extension of the boolean conjunction and are defined as binary functions $T : [0, 1]^2 \rightarrow [0, 1]$ which are commutative, associative, increasing in both variables, and 1 is its neutral element (i.e., $T(x, 1) = x$ for all $x \in [0, 1]$). Since the properties imposed in this definition are not very restrictive, there exists a lot of functions that can be used to model fuzzy conjunctions. However, in practice, the minimum $T_M(x, y) = \min\{x, y\}$ and the product $T_P(x, y) = x \cdot y$ are the preferred choice because they are easy to implement and have a simple n -ary form:

$$T_M(x_1, \dots, x_n) = \min\{x_1, \dots, x_n\}, \quad T_P(x_1, \dots, x_n) = \prod_{i=1}^n x_i.$$

In general, since all T-norms are associative, the order of the inputs does not change the output, and any t-norm defines an n -ary function which is equivalent to the iterative evaluation of each instance.

$$T(x_1, T(x_2, \dots T(x_{n-1}, x_n))) = T(x_1, \dots, x_n) = \prod_{i=1}^n x_i.$$

However, no T-norm has an easy closed expression of its n -ary form, and that is one of the reasons why the minimum and the product are mostly used. Nonetheless, continuous Archimedean T-norms are a special type that can be constructed via a unary continuous, strictly decreasing function $t : [0, 1] \rightarrow [0, +\infty)$ with $t(1) = 0$ called generator and they have a closed n -ary expression that allows a more efficient implementation Giannini et al. [2023]:

$$T(x_1, \dots, x_n) = t^{-1} \left(\min \left\{ t(0^+), \sum_{i=1}^n t(x_i) \right\} \right).$$

Any of these T-norms can be used in the FRR instead of the product to combine weights with inputs and to perform the logic inference during the second and third layers in the following manner

$$u_j^{(2)} = \sum_{v=1}^V T(f(\tilde{W}_{j,v}^{(2)})\tilde{W}_{j,v}^{(2)}, \mu_{j,v}(X_{i,j})),$$

$$u^{(3)} = \prod_{k=1}^A \sum_{j=1}^M T(f(\tilde{W}_{k,j}^{(3)})\tilde{W}_{k,j}^{(3)}, u_j^{(2)}) = \prod_{k=1}^A \sum_{j=1}^M T(f(\tilde{W}_{k,j}^{(3)})\tilde{W}_{k,j}^{(3)}, \sum_{v=1}^V T(f(\tilde{W}_{j,v}^{(2)})\tilde{W}_{j,v}^{(2)}, \mu_{j,v}(X_{i,j}))).$$

Similarly than we did in Eq. (7), if we resolve the argmax function and we take into account that $T(x, 0) = 0$ for all $x \in [0, 1]$ the truth degree of a rule r is given by

$$r(X_i) = \prod_{k=1}^A T(\tilde{W}_{k,j_k}^{(3)}, T(\tilde{W}_{j_k,v_{j_k}}^{(2)}, \mu_{j_k,v_{j_k}}(X_{i,j_k}))) = \prod_{k=1}^A T(T(\tilde{W}_{k,j_k}^{(3)}, \tilde{W}_{j_k,v_{j_k}}^{(2)}), \mu_{j_k,v_{j_k}}(X_{i,j_k})).$$

By definition, any T-norm is below the minimum $T(x, y) \leq \min\{x, y\}$, so T_M is the greatest T-norm. Then, using the minimum t-norm is the best choice to not accelerate the approach to 0 when doing the logical inference. However, the minimum only takes into account the least value of all the inputs, which may not be desirable in some cases because it may happen that the truth degrees of the fuzzy sets are neglected. Even so, there exist other families of continuously differentiable t-norms that are above the product that may help in the vanishing gradient problem, like, for instance, the family of Aczél-Alsina T-norms:

$$t_\lambda(x) = (-\log x)^\lambda, \quad T_\lambda(x_1, \dots, x_n) = e^{-\sqrt[\lambda]{\sum_{i=1}^n (-\log x_i)^\lambda}},$$

with $\lambda \in [1, +\infty)$. As $\lambda \rightarrow +\infty$, the T-norm converges to the minimum and if $\lambda = 1$ is equal to the product (see Figure 5). Also, the derivatives of different logic operators can be interpreted in terms of their contribution to the gradient van Krieken et al. [2022]. However, the use of an arbitrary T-norm may affect the explainability of the system.

D Datasets used and Code availability

The list of datasets used, alongside the number of features, samples, and classes, is in Table 3. They were collected from the UCI datasets Kelly et al. and the Keel website [Triguero et al., 2017]. The code will be publicly available on Github.

Fuzzy rule experiments using genetic optimization were carried out using the exFuzzy library [Fumanal-Idocin and Andreu-Perez, 2024], available at <https://github.com/Fuminides/ex-fuzzy>. RRL implementation is provided by the authors at <https://github.com/12wang3/rrl>. C4.5 classifier has been implemented by ourselves in Python. For the rest of the classifiers, we used the implementation available in Scikit-learn library Pedregosa et al. [2011].

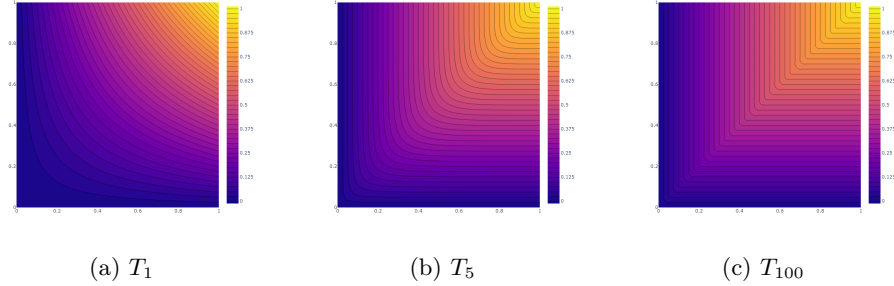


Figure 5: Contour plots of the Aczél-Alsina t-norm for different values of the parameter λ .

E Hyperparameter choosing and detailed performance for each method

We tried different configurations of hyperparameters for all the classifiers tested. The ones reported in the main text are the ones that achieved the best accuracy results for each of them.

- Random forest: we tried 100 and 200 trees with maximum depth of 3 and 5 in both cases.
- Gradient boosting: same as for random forest.
- SVM: we used two kernels, a radial basis function and a linear kernel. We also used a regularization parameter set up as 1.0 or 0.1.
- CART: we tried trees with three different cost complexity pruning parameters. The higher this parameter, the smaller the final tree shall be. We tried: 0.0, 0.001 and 0.003.
- RRL: for the RRL, we used the configurations that the authors recommend in Wang et al. [2021]. However, we obtained very similar results in all cases.
- MLP: we used three different MLPs with one, two and three hidden layers in each case. The size of the hidden layer was 100 neurons in all cases. Same for the Fuzzy MLP.
- C4.5: we tried a maximum depth of 5 and 10.

For the fuzzy classifiers trained with a genetic algorithm, we tried a different number of antecedents, rules per class and linguistic variables. The results are shown in Table 5. Figure 6 shows the same results plotted according to the complexity of each classifier according to the number of antecedents, rules and

linguistic variables used. This showcases another problem of genetic fine-tuning; it cannot find good solutions when the number of rules is high. The performance obtained in those cases is worse than the one obtained using small models.

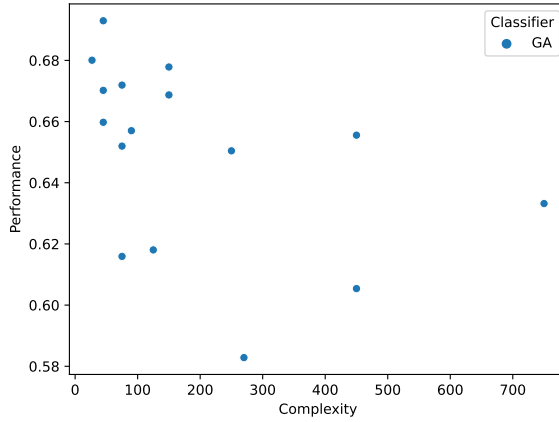
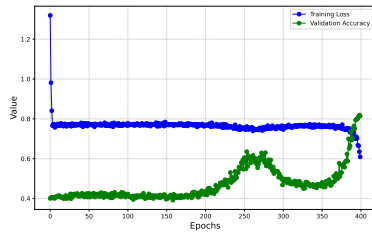


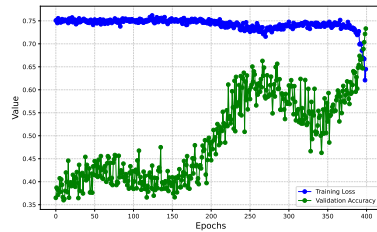
Figure 6: Relationship between complexity of the classifier and the F1 score obtained. The complexity is computed as: the number of linguistic variables * number of antecedents per rule * number of rules.

For the number of epochs, we went with 400, which was probably more than needed in most cases but did not require a significant time investment in most cases. Two examples of the evolution of loss and accuracy in training and validation, respectively, are shown in Figure 7. We can see there how the loss in training remains stable until the last epochs, where the k and γ values approach 0.

Detailed results for every classifier tested are available in Table 4.



(a) Australian dataset



(b) Magic dataset

Figure 7: Performance evolution for the FRR during two different training sessions for two datasets.

F Reducing the size of the FRR

Even though we can set up a maximum number of rules and antecedents, there are sometimes cases where the FRR can find good solutions that are considerably smaller than these specifications. In our experimentation, we found some modifications in the loss function that helped reduce the size of the rules and their number.

The strategy to shorten the rules is to add a Laplacian term in the loss function that penalizes the weights in the cancellation process that affect the antecedent truth value:

$$L_1 = \sum_{r=1}^R \sum_{k=1}^A \alpha_{k,1}^{(r)}, \quad (31)$$

which is then added to the cross-entropy loss with a multiplier, which in our experimentation was set to 0.01.

To reduce the number of rules, we use an expression taken from the Gradient boosting algorithm. The reasoning why it reduces the number of rules is not direct, but it had a clear impact on the results obtained nevertheless.

For each rule, except for the first one, we compute the residuals of the system prediction up to that rule. Then, we multiply those losses by a small factor and add it to the final loss. This works differently for sufficient and additive rules, as the final prediction is computed differently in both cases.

- For the case of sufficient rules, the loss for each rule is computed as:

$$L_r = \frac{1}{N} \sum_{i=1}^N y_i - \max_{s \in \{1, \dots, r-1\}} f(W_{s,c}^{(4)}) W_{s,c}^{(4)} r_s(X_i). \quad (32)$$

- For additive rules, we do the following:

$$L_r = \frac{1}{N} \sum_{i=1}^N y_i - \sum_{s=1}^{r-1} W_{s,c}^{(4)} r_s(X_i). \quad (33)$$

Then, we can obtain the final expression as:

$$L_2 = \sum_{r=2}^R L_r, \quad (34)$$

which can be added to the global loss as a Laplacian term. Results for the addition of this loss can be seen in Table 7. We can see there that the reduction in the number of rules is especially appreciable when the number of rules is high, even though accuracy remains mostly unaffected. For example, when using this loss, the 100 additive rules configuration reduced in 45% its number of rules.

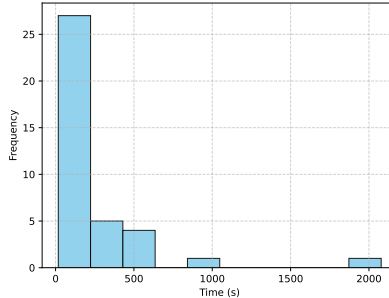


Figure 8: Histogram with execution times for all datasets using the compact FRR

G Additional configurations tested

For the sake of brevity, some of the results regarding the different gradient techniques have been cut from the main part of the manuscript, as they were not needed to draw the relevant conclusions from the experiments. However, we have included here the rest of the configurations tested in case the reader is interested in the result of a particular configuration. We show Table 6 for the ablation study in the FRR and Table 7 those for the AdFRR. Those configurations where the “K upper” and “K lower” numbers are equal to 0.0 refers to a strict indicator (k was always 0 during training in Eq. (18)). When they are both 1.0, it corresponds to the continuous indicator: $k = 1$ in Eq. (18) during the whole training.

H Computational resources employed

For the experiments using gradient-based optimization, we used the CERES cluster from the University of Essex. CERES has 1096 processing cores (2192 with hyperthreading) provided by servers with a mix of Intel E5-2698, Intel Gold 5115, 6152 and 6238L processors, and between 500Gb and 6Tb RAM each. There are also 24 NVidia GTX and RTX Series GPU cards (16 x GTX1080Ti and 8 x RTX2080). Figure 8 shows the execution time for all datasets for 400 epochs with the FRR. The average time was 218 seconds.

For the rest of the experiments, we used the Oracle Cloud Infrastructure. We set up two machines with 128GB of RAM and 32 cores.

Table 3: Datasets with their samples, features, and classes.

| Dataset | Samples | Features | Classes |
|-------------------|---------|----------|---------|
| appendicitis | 106 | 7 | 2 |
| australian | 690 | 14 | 2 |
| balance | 625 | 4 | 3 |
| banana | 5300 | 2 | 2 |
| bands | 512 | 39 | 2 |
| bupa | 345 | 6 | 2 |
| cleveland | 297 | 13 | 5 |
| coil2000 | 9822 | 85 | 2 |
| dermatology | 358 | 34 | 6 |
| glass | 214 | 9 | 6 |
| haberman | 306 | 3 | 2 |
| heart | 270 | 13 | 2 |
| hepatitis | 80 | 19 | 2 |
| housevotes | 232 | 16 | 2 |
| ionosphere | 351 | 33 | 2 |
| iris | 150 | 4 | 3 |
| magic | 19020 | 10 | 2 |
| mammographic | 830 | 5 | 2 |
| monk-2 | 432 | 6 | 2 |
| newthyroid | 215 | 5 | 3 |
| page-blocks | 5472 | 10 | 5 |
| phoneme | 5404 | 5 | 2 |
| pima | 768 | 8 | 2 |
| ring | 7400 | 20 | 2 |
| saheart | 462 | 9 | 2 |
| satimage | 6435 | 36 | 6 |
| sonar | 208 | 60 | 2 |
| spambase | 4597 | 57 | 2 |
| spectfheart | 267 | 44 | 2 |
| thyroid | 7200 | 21 | 3 |
| titanic | 2201 | 3 | 2 |
| twonorm | 7400 | 20 | 2 |
| vehicle | 846 | 18 | 4 |
| wdbc | 569 | 30 | 2 |
| wine | 178 | 13 | 3 |
| winequality-red | 1599 | 11 | 6 |
| winequality-white | 4898 | 11 | 7 |
| wisconsin | 683 | 9 | 2 |
| zoo | 101 | 16 | 7 |

Table 4: Results per each dataset obtained with the best configuration per each classifier.

| Dataset | AdFRR | FRR | LR | RF | Fuzzy MLP | GA | RLL | CART | C4.5 | SVN |
|-------------------|-------|-------|-------|-------|-----------|-------|--------|--------|--------|------|
| appendicitis | 86.36 | 77.27 | 86.36 | 84.55 | 82.73 | 90.91 | 84.03 | 79.09 | 94.02 | 76.3 |
| australian | 78.84 | 81.59 | 86.23 | 86.81 | 84.78 | 85.51 | 86.67 | 85.07 | 95.46 | 83.4 |
| balance | 79.20 | 72.80 | 88.16 | 84.16 | 78.40 | 61.60 | 84.48 | 78.56 | 73.00 | 88.4 |
| banana | 73.33 | 74.60 | 55.70 | 89.51 | 81.53 | 74.06 | 77.36 | 89.04 | 55.42 | 54.7 |
| bands | 56.43 | 59.45 | 67.12 | 72.88 | 66.58 | 64.38 | 61.64 | 63.56 | 87.55 | 69.3 |
| bupa | 70.14 | 64.64 | 68.12 | 75.36 | 72.75 | 55.07 | 65.80 | 65.51 | 66.81 | 55.0 |
| cleveland | 55.00 | 56.33 | 58.00 | 56.00 | 53.00 | 46.67 | 54.22 | 50.00 | 96.82 | 55.3 |
| coil2000 | 85.05 | 94.05 | 93.98 | 92.81 | 91.30 | 80.81 | 93.33 | 94.05 | 98.90 | 94.0 |
| dermatology | 78.05 | 74.17 | 95.56 | 97.22 | 96.11 | 50.00 | 95.53 | 94.72 | 56.05 | 97.7 |
| glass | 63.23 | 52.09 | 62.33 | 73.49 | 73.02 | 39.53 | 65.87 | 66.98 | 100.00 | 48.8 |
| haberman | 62.90 | 66.13 | 76.45 | 70.65 | 70.00 | 50.00 | 72.23 | 67.42 | 56.54 | 76.1 |
| heart | 86.29 | 81.85 | 83.70 | 82.96 | 82.96 | 70.37 | 84.81 | 73.70 | 66.17 | 77.7 |
| hepatitis | 90.00 | 85.00 | 85.00 | 88.75 | 91.25 | 81.25 | 80.00 | 82.50 | 75.89 | 86.2 |
| housevotes | 71.91 | 91.49 | 96.17 | 97.02 | 95.74 | 97.87 | 95.70 | 97.87 | 100.00 | 96.2 |
| ionosphere | 85.07 | 85.07 | 87.61 | 92.39 | 87.04 | 78.87 | 92.01 | 85.63 | 100.00 | 84.2 |
| iris | 96.66 | 94.67 | 95.33 | 96.00 | 96.67 | 76.67 | 95.33 | 96.67 | 62.50 | 96.6 |
| magic | 77.81 | 76.40 | 79.02 | 88.23 | 82.77 | 76.37 | 71.39 | 83.17 | 65.08 | 78.8 |
| mammographic | 82.77 | 82.77 | 81.33 | 80.12 | 80.96 | 77.71 | 79.88 | 82.65 | 86.04 | 77.9 |
| monk-2 | 95.17 | 82.53 | 78.62 | 98.85 | 99.54 | 63.22 | 100.00 | 100.00 | 97.10 | 82.3 |
| newthyroid | 93.48 | 86.51 | 94.88 | 96.28 | 93.02 | 88.37 | 94.88 | 93.49 | 79.56 | 88.3 |
| page-blocks | 91.01 | 91.56 | 95.95 | 97.37 | 95.95 | 92.60 | 94.63 | 96.44 | 94.74 | 92.5 |
| phoneme | 78.33 | 75.13 | 75.00 | 90.36 | 85.86 | 67.90 | 83.25 | 82.35 | 71.31 | 76.7 |
| pima | 72.59 | 73.25 | 77.66 | 77.14 | 71.43 | 74.68 | 74.08 | 71.95 | 69.24 | 76.8 |
| ring | 84.41 | 86.51 | 75.64 | 95.00 | 81.70 | 68.58 | 91.96 | 85.88 | 51.98 | 76.6 |
| saheart | 69.67 | 69.89 | 76.13 | 68.17 | 63.01 | 66.67 | 67.30 | 60.86 | 84.74 | 82.1 |
| satimage | 80.32 | 70.35 | 85.58 | 91.02 | 88.59 | 61.07 | 89.29 | 83.98 | 76.12 | 86.2 |
| sonar | 80.00 | 74.76 | 77.14 | 83.81 | 84.29 | 61.90 | 58.65 | 71.43 | 100.00 | 70.9 |
| spambase | 78.78 | 84.61 | 91.91 | 95.20 | 94.39 | 88.48 | 91.45 | 91.02 | 99.35 | 89.6 |
| spectfheart | 77.40 | 77.78 | 81.11 | 81.85 | 81.48 | 64.81 | 79.01 | 74.44 | 100.00 | 80.7 |
| thyroid | 91.52 | 92.57 | 95.65 | 99.64 | 92.86 | 88.54 | 94.51 | 99.39 | 94.01 | 93.2 |
| titanic | 75.96 | 75.42 | 77.64 | 78.91 | 78.55 | 78.91 | 77.96 | 78.37 | 78.26 | 77.5 |
| twonorm | 94.47 | 95.46 | 97.50 | 96.96 | 95.45 | 79.73 | 95.22 | 79.76 | 51.18 | 97.9 |
| vehicle | 62.27 | 53.88 | 78.82 | 74.82 | 71.18 | 52.94 | 71.52 | 68.12 | 79.62 | 69.5 |
| wdbc | 94.91 | 92.11 | 97.54 | 96.49 | 96.67 | 89.47 | 95.26 | 94.04 | 84.61 | 97.1 |
| winequality-red | 54.62 | 49.38 | 59.56 | 67.62 | 59.38 | 23.12 | 59.66 | 59.31 | 52.39 | 58.7 |
| winequality-white | 49.91 | 40.06 | 53.73 | 66.47 | 59.59 | 20.61 | 54.10 | 52.47 | 50.12 | 51.0 |
| wine | 97.22 | 95.00 | 98.89 | 97.78 | 97.78 | 91.67 | 96.60 | 92.22 | 70.79 | 98.3 |
| wisconsin | 97.51 | 93.72 | 96.50 | 96.93 | 96.20 | 95.62 | 95.32 | 94.74 | 98.62 | 97.3 |
| zoo | 42.85 | 60.95 | 91.43 | 96.19 | 95.24 | 71.43 | 93.00 | 95.24 | 100.00 | 94.9 |

Table 5: Results for genetic fine tuning of rules with linguistic hedges.

| Rules per class | Antecedents | Linguistic variables | Acc. | F1 score |
|-----------------|-------------|----------------------|-------|----------|
| 3 | 3 | 3 | 70.14 | 68.00 |
| 3 | 3 | 5 | 69.18 | 67.02 |
| 3 | 5 | 3 | 68.89 | 65.97 |
| 3 | 5 | 5 | 65.78 | 61.59 |
| 5 | 3 | 3 | 70.67 | 69.29 |
| 5 | 3 | 5 | 69.31 | 67.19 |
| 5 | 5 | 3 | 67.27 | 65.19 |
| 5 | 5 | 5 | 65.00 | 61.80 |
| 10 | 3 | 3 | 67.89 | 65.35 |
| 10 | 3 | 5 | 69.24 | 66.87 |
| 10 | 5 | 3 | 69.68 | 67.78 |
| 10 | 5 | 5 | 67.17 | 65.04 |
| 30 | 3 | 3 | 62.14 | 58.28 |
| 30 | 3 | 5 | 63.95 | 60.53 |
| 30 | 5 | 3 | 68.30 | 65.55 |
| 30 | 5 | 5 | 65.99 | 63.32 |

Table 6: Summary of results for different configurations of gradient strategies for the FRR.

| Rules | Antecedents | LV | Sufficient | Grad mode | K upper train | K lower train | Temp | Residual | Boosted loss | Acc - GA Acc | Acc - LR Acc | N rules | N ants | Acc |
|-------|-------------|----|------------|------------------|---------------|---------------|------|----------|--------------|--------------|--------------|---------|--------|-------|
| 15 | 3 | 3 | True | STEO | 0.0 | 0.0 | 0.1 | True | False | 6.45 | -5.22 | 13.81 | 1.86 | 76.91 |
| 15 | 3 | 3 | True | GRAFT | 1.0 | 0.0 | 0.1 | True | False | 6.33 | -5.34 | 12.57 | 1.91 | 76.79 |
| 15 | 3 | 3 | True | STE ₁ | 1.0 | 1.0 | 0.1 | True | False | 6.25 | -5.42 | 13.78 | 1.84 | 76.71 |
| 15 | 3 | 3 | True | GRAFT | 0.0 | 0.0 | 0.1 | True | False | 6.22 | -5.45 | 13.80 | 1.89 | 76.68 |
| 15 | 3 | 3 | True | STE ₁ | 0.0 | 0.0 | 0.1 | True | False | 6.17 | -5.50 | 13.74 | 1.88 | 76.63 |
| 15 | 3 | 3 | True | STE ₁ | 1.0 | 0.0 | 0.1 | True | False | 5.95 | -5.72 | 13.56 | 1.84 | 76.41 |
| 15 | 3 | 3 | True | GRAFT | 1.0 | 1.0 | 0.1 | True | False | 5.51 | -6.16 | 12.66 | 1.93 | 75.97 |
| 15 | 3 | 3 | True | STEO | 1.0 | 0.0 | 0.1 | True | False | 4.70 | -6.97 | 13.78 | 1.85 | 75.16 |
| 15 | 3 | 3 | True | GRAFT | 1.0 | 0.0 | 0.1 | False | False | 3.62 | -8.05 | 12.92 | 1.90 | 74.08 |
| 15 | 3 | 3 | True | STEO | 1.0 | 1.0 | 0.1 | False | False | 3.43 | -8.24 | 13.89 | 1.83 | 73.89 |
| 15 | 3 | 3 | True | STEO | 0.0 | 0.0 | 0.1 | False | False | 3.34 | -8.33 | 13.87 | 1.78 | 73.80 |
| 15 | 3 | 3 | True | STEO | 0.0 | 0.0 | 0.1 | False | False | 3.00 | -8.67 | 13.94 | 1.78 | 73.47 |
| 15 | 3 | 3 | True | STEO | 1.0 | 0.0 | 0.1 | False | False | 2.49 | -9.17 | 13.98 | 1.81 | 72.96 |
| 15 | 3 | 3 | True | GRAFT | 1.0 | 1.0 | 0.1 | False | False | 2.35 | -9.31 | 12.82 | 1.95 | 72.82 |
| 15 | 3 | 3 | True | STEO | 1.0 | 1.0 | 0.1 | False | False | -14.94 | -26.61 | 12.77 | 1.87 | 55.52 |

Table 7: Comparison of different AdFRR configurations and their accuracies.

| Rules | Antecedents | LV | Sufficient | Grad mode | K upper train | K lower train | Temp | Residual | Boosted loss | Acc - GA Acc | Acc - LR Acc | N rules | N ants | Acc |
|-------|-------------|----|------------|-----------|---------------|---------------|------|----------|--------------|--------------|--------------|---------|--------|-------|
| 70 | 3 | 3 | False | STEO | 1.0 | 0.0 | 0.1 | True | False | 75.40 | 04.12 | 50.04 | 1.88 | 78.00 |
| 70 | 3 | 3 | False | STEO | 1.0 | 0.0 | 0.1 | True | True | 69.01 | 04.76 | 32.32 | 1.32 | 77.36 |
| 100 | 3 | 3 | False | STEO | 1.0 | 0.0 | 0.1 | True | False | 67.22 | 04.94 | 66.21 | 1.94 | 77.18 |
| 100 | 3 | 3 | False | STEO | 1.0 | 0.0 | 0.1 | True | True | 59.26 | 05.74 | 36.14 | 1.30 | 76.38 |
| 50 | 3 | 3 | False | STEO | 1.0 | 0.0 | 0.1 | True | False | 58.94 | 05.77 | 37.76 | 1.82 | 76.35 |
| 50 | 3 | 3 | False | STEO | 1.0 | 0.0 | 0.1 | True | True | 58.77 | 05.79 | 27.54 | 1.34 | 76.33 |
| 30 | 3 | 3 | False | STEO | 1.0 | 0.0 | 0.1 | True | True | 50.07 | 06.66 | 21.22 | 1.39 | 75.46 |
| 30 | 3 | 3 | False | STEO | 1.0 | 0.0 | 0.1 | True | False | 48.33 | 06.83 | 21.43 | 1.75 | 75.29 |
| 15 | 3 | 3 | False | STEO | 1.0 | 0.0 | 0.1 | True | False | 26.80 | 08.98 | 13.62 | 1.74 | 73.14 |
| 15 | 3 | 3 | False | STEO | 1.0 | 0.0 | 0.1 | True | True | 15.15 | 10.15 | 13.01 | 1.44 | 71.97 |